Host JAK-STAT activity is a target of parasitoid wasp virulence strategies

Authors: Susanna E. Brantley[1], Corinne M. Stouthamer[2], Pooja Kr[3], Mary L. Fischer[3], Joshua Hill[3], Todd A. Schlenke[2], Nathan T. Mortimer[3,4]

Affiliations: [1]Department of Cell Biology, Duke University Medical Center, Durham, NC 27705, USA; [2]Department of Entomology, University of Arizona, Tucson, AZ 85719, USA; [3]School of Biological Sciences, Illinois State University, Normal, IL 61790, USA; [4]Department of Biochemistry & Biophysics, Oregon State University, Corvallis, OR 97330, USA

Corresponding authors:

Nathan T. Mortimer, nathan.mortimer@oregonstate.edu, Department of Biochemistry & Biophysics, Oregon State University, Corvallis, OR 97330, USA

Todd A. Schlenke, schlenke@email.arizona.edu, Department of Entomology, University of Arizona, Tucson, AZ 85719, USA

Short title: JAK-STAT signaling and parasitoid virulence

Abstract

Innate immune responses that allow hosts to survive infection depend on the action of multiple conserved signaling pathways. Pathogens and parasites in turn have evolved virulence factors to target these immune signaling pathways in an attempt to overcome host immunity. Consequently, the interactions between host immune molecules and pathogen virulence factors play an important role in determining the outcome of an infection. The immune responses of *Drosophila melanogaster* provide a valuable model to understand immune signaling and host-pathogen interactions. Flies are commonly infected by parasitoid wasps and mount a coordinated cellular immune response following infection. This response is characterized by the production of specialized blood cells called lamellocytes that form a tight capsule around wasp eggs in the host hemocoel. The conserved JAK-STAT signaling pathway has been implicated in lamellocyte proliferation and is required for successful encapsulation of wasp eggs. Here we show that activity of *Stat92E*, the *D. melanogaster* STAT ortholog, is induced in immune tissues following parasitoid infection. Virulent wasp species are able to suppress *Stat92E* activity during infection, suggesting they target JAK-STAT pathway activation as a virulence strategy. Furthermore, two wasp species (*Leptopilina guineaensis* and *Ganaspis xanthopoda*) suppress phenotypes associated with a gain-of-function mutation in *hopscotch*, the *D. melanogaster* JAK ortholog, indicating that they inhibit the activity of the core signaling components of the JAK-STAT pathway. Our data suggest that parasitoid wasp virulence factors block JAK-STAT signaling to overcome fly immune defenses.

Author Summary

Following infection, host immune responses are triggered to provide protection against the invading pathogen. The proper function of these responses depends on the activity of multiple immune signaling pathways. These pathways act in a coordinated manner to orchestrate the immune response, and any disruption can render the host susceptible to infection. Because of this sensitivity, many pathogen species have evolved virulence mechanisms that target host signaling pathways and disrupt their function. We are using the interaction between *Drosophila melanogaster* and *Drosophila*-infecting parasitoid wasps to study this relationship between host signaling and pathogen virulence. Parasitoids infect fly larvae, and during infection, transfer virulence protein containing venom into the host, providing a mechanism to alter host signaling. This study is focused on one key immune signaling pathway, the highly conserved JAK-STAT pathway. We find that many virulent parasitoid species restrict the activity of the host JAK-STAT pathway, providing a clue as to their virulence strategy. JAK-STAT signaling plays many additional roles in health and disease, and so this system provides a good model to further understand this important pathway.

INTRODUCTION

Innate immune mechanisms are evolutionarily ancient host defenses against invading pathogens. These innate mechanisms include both humoral and cell-mediated responses to infection and are coordinated by numerous immune signaling pathways [1]. Many of these pathways are highly conserved across taxa [2,3], including the signaling pathways underlying humoral responses such as the Toll/Toll-like Receptor pathway [4–7], and the pathways involved in cell-mediated immunity such as JAK-STAT, JNK and calcium signaling [8–13]. Following infection, the coordinated function of these signaling pathways is required for host resistance to infection [14,15]; the activation, duration and strength of each signaling event is therefore tightly regulated, and dysregulated immune signaling can result in immune deficiency [16–18]. In turn, pathogens have evolved an array of virulence factors that allow them to subvert host immune responses [19–21]. Conserved immune signaling pathways are commonly targeted by pathogen virulence factors across diverse host and pathogen taxa [12,22–26], reflecting their important role in host defense.

Drosophila melanogaster is a commonly used model of human health and disease, and studies into fly immunity have been key to understanding innate immune signaling [27–29]. Flies are naturally infected by a wide range of pathogens including microbes, viruses and macroparasites, and mount specific responses to each class of pathogen [30]. Parasitoid wasps are a common macroparasite of *Drosophila* species, and the *Drosophila*-parasitoid system has been used as a model to study the co-evolution and molecular mechanisms underlying host-parasite interactions [31–35]. Numerous parasitoid wasp species infect flies in nature, and during infection these wasps inject an egg along with virulence factor containing venom into the hemocoel of

fly larvae. This triggers a host cellular immune response known as encapsulation [32,36]. In the cellular encapsulation response, circulating macrophage-like hemocytes known as plasmatocytes are activated by parasitoid infection and become the first hemocytes to encounter and bind to the foreign tissue [12,37]. Infection also triggers the production of lamellocytes, an induced hemocyte type that is required for the encapsulation of parasitoid eggs and other pathogens that are too large to be phagocytosed [38]. These specialized hemocytes can be derived from hemocyte precursors in the hematopoietic lymph gland as well as from the transdifferentiation of circulating and sessile plasmatocytes, via an intermediate prelamellocyte form (also known as podocytes or lamellocyte intermediates) [39–45]. Following their production, lamellocytes migrate towards and spread over the foreign tissue, forming a continuous capsule and killing the encapsulated object [37,46,47].

Our understanding of the encapsulation process is incomplete, but it is becoming increasingly apparent that the regulation of this cellular response relies on conserved signaling mechanisms that are likely important for human immunity [46,48,49]. One such signaling pathway, the JAK-STAT pathway (Fig 1A), is linked with the cellular encapsulation response against macroparasite infection [49,50] and plays a conserved role in immune responses across a wide range of organisms [8,9,51]. In *D. melanogaster,* JAK-STAT pathway activation is initiated by the production and release of cytokines from the *unpaired* (*upd*) family: *upd1, upd2*, and *upd3* [52–55]. *Upd* proteins are secreted cytokines that bind to and activate the *domeless* (*dome*) cytokine receptor [53,56]. Activation of *dome* triggers the activity of the Janus Kinase (JAK) ortholog *hopscotch* (*hop*), which in turn phosphorylates the Signal Transducer and Activator of Transcription (STAT) ortholog *Stat92E* [53,56,57]. Phosphorylated *Stat92E* can then enter the nucleus to drive transcription of downstream target genes [57–59], leading to

the production of lamellocytes and other signaling outputs. The production of lamellocytes is linked with JAK-STAT activity both in response to macroparasite infection [49,50], and also as a consequence of gain-of-function mutations in *hop* or *Stat92E,* which cause the precocious differentiation of lamellocytes in naïve flies [60–63]. Conversely, loss-of-function mutations in *hop* lead to reduced hemocyte counts and weakened encapsulation ability [49].

Drosophila-infecting parasitoid species have evolved diverse venom-mediated virulence strategies to overcome host immunity, and many of these mechanisms target host hemocyte production or function [12,26,64–71]. Notably, multiple species of *Drosophila*-infecting parasitoids employ venom factors that specifically target host lamellocytes [38,46,71–75], suggesting that inhibition of the production or activity of lamellocytes may be an effective parasitoid virulence strategy. Based on these data, we predict that parasitoids might suppress host lamellocyte production and encapsulation by specifically targeting the JAK-STAT pathway. In this study, we show that a panel of virulent parasitoid wasp species suppress JAK-STAT pathway activity following infection. We find that parasitoids likely target the JAK-STAT pathway through distinct mechanisms, with different species inhibiting either the upstream activation or the activity of the core signaling components of the pathway. Our findings demonstrate that parasite virulence mechanisms have converged on a strategy of host JAK-STAT activity disruption.

RESULTS

JAK-STAT pathway activation following parasitoid infection

To characterize the tissue specificity of JAK-STAT pathway activation in the context of the immune response to wasp infection, we assayed pathway activity using *Stat92E* activity reporter flies (*10XStat92E-GFP*) [76] in naïve larvae, and larvae infected with an avirulent parasitoid wasp. *10XStat92E-GFP* flies express GFP in response to JAK-STAT pathway activation (Fig 1A) such that GFP fluorescence can be used as a relative measure of pathway activity [76]. In naïve reporter flies, GFP expression was observed in cells of the gut (Fig S1A), but no expression was observed in immune tissues such as the hemocytes (Fig 1B-C), fat body (Fig 1D), body wall muscle (Fig 1E) or lymph gland (Fig S1B). To characterize reporter expression following infection, we challenged *10XStat92E-GFP* larvae with the avirulent parasitoid *Leptopilina clavipes* (strain LcNet), a species that induces a robust immune response and is usually encapsulated by *D. melanogaster* [46]. We found that LcNet infection alters the pattern of *10XStat92E-GFP* activity: at 48 hours post infection (hpi), GFP fluorescence was detected in hemocytes (Fig 1F-G), fat body (Fig 1H), and body wall muscles (Fig 1I), but not in the lymph gland (Fig S1C). These data suggest that JAK-STAT signaling in these tissues may play an important role in the host encapsulation response to macroparasite infection.

Lamellocyte production and changes to hemocyte concentration are induced by JAK-STAT activity in diverse tissues

D. melanogaster resistance to parasitoid infection is influenced by the total number of circulating hemocytes, the induction of lamellocytes, and also the concentrations of hemocyte types following infection [49,77–80]. To investigate the tissue specific roles of JAK-STAT activity in inducing changes in the host hemocyte population, we expressed a constitutively active form of *Stat92E* (*Stat92E*^{CA}) [63] in

immune tissues using the *UAS-GAL4* system [81]. Specifically, we expressed *Stat92E*^{CA} in hemocytes using *He-Gal4*, in fat body using *C833-Gal4*, in body wall muscle using *Mef2-Gal4*, in the Posterior Signaling Center (PSC) of the lymph gland using *Dot-Gal4*, and in the Medullary zone (MZ) of the lymph gland using *unc-5*^{GMR93E08} (hereafter referred to as *MZ-Gal4*) [62,82–85]. For each experiment we determined the number of each type of circulating hemocyte. The effect of *Gal4* expression was controlled for by outcrossing each *Gal4* line to the *w*^{1118} genetic background control.

We found that hemocyte-specific expression of *Stat92E*^{CA} failed to induce an increase in the total number of circulating hemocytes (Fig 2A), but that this expression led to a significant increase in the number of lamellocytes (Fig 2B). To further explore the effect of JAK-STAT signaling in hemocytes, we used the χ^2 test to determine whether the expression of *Stat92E*^{CA} in hemocytes altered the observed distribution of hemocytes across each type compared to the expected numbers calculated from the background control. We found that *Stat92E*^{CA} expression had a significant effect on the concentration of hemocyte types (χ^2 = 548.8, p = 4.99 x 10^{-4}). To investigate the effect on each hemocyte type we plotted the χ^2 residuals for each cell type (Fig 2C), as a measure of the contribution of each cell type to the overall effect. This demonstrates that the concentration of plasmatocytes is decreased in these larvae coincident with an increase in the concentration of prelamellocytes and lamellocytes, suggesting that *Stat92E*^{CA} expression in hemocytes is driving the transdifferentiation of plasmatocytes into lamellocytes via the prelamellocyte intermediate stage, as is also observed following parasitoid infection [39] or upon organism-wide JAK-STAT activation [45].

Further, we found that expression of *Stat92E*^{CA} in the fat body, the major site of humoral immune signaling, promoted lamellocyte differentiation without significant

changes to the total number of circulating hemocytes (Fig 2A-B). Fat body expression of *Stat92E*^{CA} also altered the overall concentration of hemocytes ($\chi^2 = 23.41$, $p = 1.99 \times 10^{-3}$). In contrast to the case of *Stat92E*^{CA} expression in hemocytes, this alteration in the fat body appeared to be driven solely by an increase in lamellocytes (Fig 2C). This suggests that fat body expression of *Stat92E*^{CA} may induce the production of lamellocytes from non-circulating precursor cells. These contradictory results may be reconciled by considering that the number of lamellocytes produced is markedly less when *Stat92E*^{CA} is expressed in fat body in comparison with hemocyte expression. Following fat body *Stat92E*^{CA} expression, lamellocytes only account for 1.3% of the circulating hemocytes. This modest increase may not be sufficient to significantly impact the total number of hemocytes, and indeed we see that fat body *Stat92E*^{CA} expression caused a small, but not statistically significant increase in hemocyte number ($379.0 \pm 44.1 \times 10^4$ hemocytes/ml in *Stat92E*^{CA} expression compared to $328.2 \pm 22.5 \times 10^4$ hemocytes/ml in control, $p = 0.189$). This suggests that the contribution of fat body signaling to lamellocyte production is limited, perhaps explaining why inhibition of JAK-STAT signaling in the fat body has minimal consequences for host defense following infection [50].

The larval body wall muscle has recently been shown to play a vital role in host defense to parasitoid infection, an effect mediated by JAK-STAT signaling [50]. Accordingly, we found that muscle-specific expression of *Stat92E*^{CA} with the *Mef2-Gal4* driver was sufficient to induce both an increase in the total number of circulating hemocytes (Fig 2A) and the production of lamellocytes (Fig 2B), and altered the overall proportion of cell types in the hemocyte population ($\chi^2 = 203.6$, $p = 5.0 \times 10^{-4}$). The increase in total circulating hemocytes suggests that muscle JAK-STAT activity is likely triggering the production of hemocytes via the release from sessile hemocyte

populations or the lymph gland into circulation. These newly produced hemocytes are likely differentiating into lamellocytes as reflected by the increased lamellocyte numbers and increases in the concentrations of both prelamellocytes and lamellocytes (Fig 2C).

Finally, we expressed *Stat92E*^{CA} in two distinct cell populations within the lymph gland: the PSC and MZ. We found that *Stat92E*^{CA} expression in either of these lymph gland cell types did not induce an increase in hemocyte number or lamellocyte production (Fig 2A-B), nor did it alter the concentration of hemocyte types in circulation (*Dot-Gal4:* χ^2 = 1.467, p = 0.42; *MZ-Gal4*: χ^2 = 2.549, p = 0.28) (Fig 2C). This is consistent with the described role of JAK-STAT signaling in restricting hematopoiesis within the lymph gland [86–88], and the lack of pathway activity in lymph gland cells following infection (Fig S1C).

The virulence mechanisms of multiple parasitoid species target the JAK-STAT pathway

To test whether *Drosophila*-infecting parasitoid species can manipulate host JAK-STAT signaling, we challenged *Stat92E* activity reporter flies (*10XStat92E-GFP*) with a panel of diverse wasp species and strains (Fig S2). We found that immune challenge induced wasp-specific patterns of *10XStat92E-GFP* activity in hemocytes (Fig 3A-B), fat body (Table 1 and Fig S3), and body wall muscle (Table 2 and Fig S4) at 24hpi and 48hpi. Infection with two species of avirulent wasps, *Leptopilina clavipes* (strain LcNet) and *Leptopilina maia* (strain LmAtl) [89,90] both induce a high level of *10XStat92E-GFP* activity in hemocytes (Fig 3A-B), fat body (Table 1) and body wall muscle (Table 2).

Table 1. *10XStat92E-GFP* activity in fat body following wasp infection by multiple wasp strains. (-, +, ++) indicates estimated observed fluorescence intensity. Examples of qualitative levels of GFP fluorescence are shown in Fig S3.

Treatment	24h post-infection	48h post-infection
Naïve	-	-
Lb17	+	+
LbG486	+	+
Lh14	-	-
LhSw	-	-
LgCam	++	++
LgSA	-	-
LvPhil	-	+
LvHaw	-	+
LcNet	++	++
LmAtl	++	++
GxUg	-	-
GxHaw	-	-

Table 2. *10XStat92E-GFP* activity in body wall muscle tissue following wasp infection by multiple wasp strains. (-, +, ++) indicates estimated observed fluorescence intensity. Examples of qualitative levels of GFP fluorescence are shown in Fig S4.

Treatment	24h post-infection	48h post-infection
Naïve	-	-
Lb17	-	-
LbG486	-	-
Lh14	-	-
LhSw	-	-

LgCam	-	-
LgSA	-	-
LvPhil	-	-
LvHaw	-	-
LcNet	++	++
LmAtl	++	++
GxUg	+	+
GxHaw	-	-

In hemocytes, the levels of *10XStat92E-GFP* activity were highly induced at 24hpi (Fig 3A) following LmAtl and LcNet infection, and although they began to decrease, remained significantly elevated at 48hpi (Fig 3B). In contrast, infection with multiple strains of the virulent parasitoid species *Ganaspis xanthopoda*, *Leptopilina boulardi*, *Leptopilina guineaensis*, *Leptopilina victoriae* and *Leptopilina heterotoma* [33,46,75,78,91] induced lower levels of GFP fluorescence in hemocytes 24hpi (Fig 3A) and 48hpi (Fig 3B). GFP fluorescence levels in hemocytes from *10XStat92E-GFP* larvae infected with either of two strains of *L. guineaensis* (LgCam and LgSA) or *L. heterotoma* (Lh14 and LhSw) were indistinguishable from naïve controls at both time points, suggesting that the venoms of these wasps are either able to prevent the upstream activation of the JAK-STAT pathway or to inhibit the activity of the core signaling components following pathway activation in hemocytes. A moderate level of *10XStat92E-GFP* fluorescence was induced in hemocytes following infection by at least one strain of *G. xanthopoda* (GxHaw), *L. boulardi* (Lb17) or *L. victoriae* (LvHaw), but these levels were significantly lower than those induced by *L. clavipes* infection (GxHaw: $t = -7.91$, $p < 1.0 \times 10^{-4}$; Lb17: $t = -4.83$, $p < 1.0 \times 10^{-4}$; LvHaw: $t = -4.83$, $p < 1.0 \times 10^{-4}$, all compared with LcNet at 48hpi). These data suggest that venoms from these virulent

wasp strains are able to limit JAK-STAT pathway activity in host hemocytes to below the levels induced by infection with an avirulent species.

In the fat body (Table 1), infection by LgCam induced a comparable level of *10XStat92E-GFP* activity to infection by the avirulent strains LcNet or LmAtl. Interestingly, a second strain of *L. guineaensis* (LgSA) did not induce GFP fluorescence in the fat body, underlining the potential differences in virulence mechanisms between strains [34,92]. Infection by either of two strains each of *L. boulardi* (Lb17 and LbG486) and *L. victoriae* (LvPhil and LvHaw) led to a low level of GFP fluorescence in the fat body following infection, but infection by the other virulent parasitoid species did not induce fat body *10XStat92E-GFP* activity, suggesting that these wasps inhibit JAK-STAT activation in this tissue.

In the body wall muscle (Table 2), infection by *G. xanthopoda* strain GxUg induced a moderate level of *10XStat92E-GFP* activity. With the exception of GxUg, none of the other virulent parasitoid species, including the *G. xanthopoda* strain GxHaw, induced a visible level of GFP fluorescence in the body wall muscle following infection. In contrast, avirulent strains LcNet and LmAtl resulted in strong *10XStat92E-GFP* activity. Again, this suggests that the activation of the JAK-STAT pathway in body wall muscle is targeted by the venoms of these virulent parasitoid wasp species.

Parasitoid virulence mechanisms target JAK-STAT at distinct steps of pathway activation

Our results show that JAK-STAT signaling is active in immune tissues following parasitoid infection and suggest that it can be modulated by wasp virulence

mechanisms. Next, we wanted to test whether these parasitoid species are inhibiting the activation of the JAK-STAT pathway or the function of the core pathway components downstream of activation. To differentiate between these possibilities, we used the *hop* gain of function mutant fly strain, hop^{Tum} [61]. hop^{Tum} is a temperature-sensitive gain of function mutation, such that at restrictive temperatures *hop* activation becomes independent of upstream signaling leading to elevated JAK-STAT signaling even in the absence of pathway induction by *upd* cytokines [60]. This results in the production of large numbers of lamellocytes in naïve flies [57]. Lamellocytes are adhesive cells, and in the absence of parasitoid eggs or another target for encapsulation in hop^{Tum} mutants, they bind to each other resulting in melanized cell nodules that are often referred to as "melanotic tumors" (Fig 4A) [93]. Because hop^{Tum} mutants express a constitutively active form of JAK, we predict that parasitoid species that inhibit pathway activation upstream of JAK would have no effect on the melanotic tumor phenotype, whereas parasitoid species that block the function of the core components of the pathway would suppress the melanotic tumor phenotype.

We infected hop^{Tum} flies with the panel of wasp species and strains and observed the effect of wasp infection on the penetrance of the melanotic tumor phenotype. Infection by multiple strains of two wasp species, *L. guineaensis* (LgCam and LgSA) and *G. xanthopoda* (GxUg and GxHaw) significantly reduced the penetrance of the melanotic tumor phenotype in hop^{Tum} flies (Fig 4B). These findings suggest that the virulence mechanisms of *L. guineaensis* and *G. xanthopoda* may act by inhibiting JAK-STAT pathway function downstream of activation.

We further explored this idea focusing on the virulent *L. guineaensis* strain LgCam. LgCam infection led to a significant decrease both in tumor penetrance in the

hop^{Tum} mutant background (Fig 4B), and in *10XStat92E-GFP* activity in hemocytes (Fig 3A-B) and body wall muscle (Table 2). To test the hypothesis that LgCam venom blocks JAK-STAT function downstream of pathway activation, we incubated primary hemocyte cultures derived from *hop*^{Tum}*; 10XStat92E-GFP* larvae with purified LgCam venom in phosphate buffered saline (PBS). Hemocytes from these larvae have constitutively elevated JAK-STAT activity and *10XStat92E-GFP* expression, and we predict that if LgCam venom is sufficient to block JAK-STAT pathway activity downstream of *hop* activation, then we will see decreased GFP fluorescence in hemocytes incubated with LgCam venom compared to hemocytes incubated with PBS control. We found that 1 hour of LgCam venom incubation was sufficient to significantly lower GFP fluorescence intensity compared to incubation with PBS alone ($F = 13.2$, $p = 3.4 \times 10^{-4}$) (Fig 4C). This suggests that LgCam venom components are inhibiting JAK-STAT via core pathway activity, rather than through an indirect effect of infection or pathway activation.

To test whether this JAK-STAT inhibition contributes to parasitoid success, we expressed *Stat92E*^{CA} in hemocytes and measured the encapsulation rate of LgCam eggs. If LgCam virulence is dependent on inhibiting JAK-STAT pathway activity in hemocytes, we would expect that *Stat92E*^{CA} expression would confer some degree of host resistance. We found that while none of the eggs in control larvae were encapsulated, flies expressing *Stat92E*^{CA} in hemocytes showed a significantly increased rate of LgCam encapsulation ($F = 36$, $p = 3.88 \times 10^{-3}$) (Fig 4D). This supports the idea that LgCam virulence targets core JAK-STAT pathway function, likely at the level of *Stat92E* activity.

Suppression of the *hop*^{Tum} melanotic tumor phenotype is correlated with alterations to the circulating hemocyte population

To determine how the virulence strategies of these virulent parasitoid species affect hemocyte production in *hop*^{Tum} larvae, we measured the numbers of the different hemocyte types at 48hpi. In wild type flies infected by the avirulent parasitoid strain LcNet, increased numbers of lamellocytes are observed at 48hpi [46]. We found that LcNet infection also induced higher numbers of circulating lamellocytes in the *hop*^{Tum} background compared to naïve *hop*^{Tum} larvae ($t = 2.85$, $p = 0.03$) (Fig 4E-F), indicating that *hop*^{Tum} mutants are still capable of responding to parasitoid infection by elevating lamellocyte numbers. We found that infection with strains of *L. guineaensis* and *G. xanthopoda* did not lead to a decrease in the total number of circulating hemocytes (Fig 4E). However, we found that infection by the *G. xanthopoda* strain GxUg led to a significant decrease in lamellocyte numbers in infected *hop*^{Tum} mutant larvae ($t = -2.89$, $p = 0.047$) (Fig 4F). Infection by the closely related strain GxHaw and the *L. guineaensis* strains LgCam and LgSA also led to a consistent decrease in lamellocyte numbers (Fig 4F), although these values were not below an α value of 0.05 (GxHaw: $t = -1.65$, $p = 0.104$; LgCam: $t = -2.133$, $p = 0.082$; LgSA: $t = -1.56$, $p = 0.106$).

Based on previous findings that the concentration of hemocyte types in circulation is an important factor in host defense [49] and our observation that ectopic JAK-STAT expression in immune tissues altered this concentration (Fig 2C), we hypothesized that there may be a correlation between melanotic tumor penetrance and the concentration of hemocyte types. We determined the proportion of each hemocyte type in *hop*^{Tum} larvae infected by all parasitoid species and strains and tested for a correlation between these proportions and the penetrance of melanotic tumor phenotype following the respective infection. We found that relative numbers of plasmatocytes ($\rho = -0.033$, $p = 0.915$) (Fig 5A) or prelamellocytes ($\rho = -0.341$, $p = 0.255$) (Fig 5B) were not

correlated with *hop*^{Tum} melanotic tumor penetrance. However, we found a significant correlation between relative lamellocyte numbers and melanotic tumor phenotype penetrance (ρ = 0.555, p = 0.025) (Fig 5C), in which high tumor penetrance was associated with a higher proportion of circulating lamellocytes.

DISCUSSION

Our data demonstrate that the JAK-STAT signaling pathway is active in *D. melanogaster* immune tissues following parasitoid wasp infection and that pathway activity in these tissues can induce the production of lamellocytes, likely via distinct mechanisms. JAK-STAT activation in hemocytes, via the hemocyte-specific expression of the constitutively active *Stat92E*^{CA}, led to the production of lamellocytes without an increase in the overall circulating hemocyte count. Previous studies that have shown through lineage tracing experiments that a subset of plasmatocytes transdifferentiate into lamellocytes as part of the immune response against parasitic wasps [39,40,45]. Our data suggest that this transdifferentiation may be stimulated by JAK-STAT activity specifically in hemocytes.

In agreement with recent work [50], we found that expression of *Stat92E*^{CA} in the body wall muscle using the *Mef2-Gal4* driver induced an overall increase in the number of circulating hemocytes and the production of lamellocytes, suggesting that JAK-STAT activity in the body wall muscle may act through a non-autonomous signaling mechanism to induce the production of new hemocytes that differentiate into lamellocytes. We observe a similar trend when *Stat92E*^{CA} expression is driven in the fat body by *C833-Gal4*, although far fewer lamellocytes were produced and the increase in hemocyte numbers did not reach significance. The origin of the *de novo* lamellocyte

population following JAK-STAT activation in the body wall muscle or fat body is unclear from these data, but two hypotheses can be suggested. First, lamellocytes can be produced in the lymph gland from prohemocytes [94]. Perhaps a cytokine signal downstream of JAK-STAT activation is secreted from peripheral tissues to stimulate lamellocyte differentiation and release of new hemocytes into circulation from the lymph gland. A second hypothesis is that a cytokine produced by JAK-STAT signaling in the body wall muscle or fat body is received by the sessile hemocyte population. These blood cells are found adjacent to the body wall muscle and remain out of circulation in wild type, naïve flies. When marked with GFP, these cells can be observed as a distinct banding pattern on the fly cuticle [95,96]. However, upon wasp infection, this banding pattern disappears, suggesting that the sessile hemocytes have entered circulation [42,62]. Differentiation of these cells into lamellocytes may be the source of the excess lamellocytes we observed following expression of *Stat92E*^{CA} in the body wall muscle or fat body.

Consistent with the induction of lamellocyte differentiation by *Stat92E*^{CA} expression, we found that wasp infection led to JAK-STAT activity in the hemocytes, body wall muscle, and fat body. The requirement for JAK-STAT activity in the encapsulation response [49,50] suggests that the pathway could be a likely target for wasp virulence factors, and indeed we found that the virulent wasp strains we tested seemed to induce lower levels of JAK-STAT activity in the immune tissues of their fly hosts than the avirulent wasp strains LcNet and LmAtl. Based on our observations, we conclude that this pathway inhibition may take on several forms. For instance, in hemocytes, strains of *L. guineaensis* and *L. heterotoma* suppress JAK-STAT signaling to the level of naïve flies, suggesting a complete inhibition of pathway activation or function. On the other hand, hemocytes infected by GxHaw induced a peak of signaling at 24hpi

but were indistinguishable from naïve flies by 48hpi, suggesting that GxHaw infection may act to shorten the duration of pathway activity. Conversely, JAK-STAT signaling in hemocytes of Lb17 and LvHaw infected flies was not active at 24hpi but showed elevated signaling at 48hpi. This is potentially indicative of a delay in pathway activation. Similar effects were seen in the ability of virulent wasps to manipulate host JAK-STAT activity in body wall muscle and fat body, although such patterns are more difficult to discern from qualitative data. The virulence of these wasp species suggests that along with the strength of pathway activity, the timing and duration of JAK-STAT signaling may also play a key role in host resistance.

The functional significance of the ability of wasps to target the JAK-STAT pathway as a virulence mechanism is evident in our observation that flies with overactive JAK-STAT pathway activity in hemocytes are less susceptible to the virulent wasp LgCam. The resistance conferred by *Stat92E*^{CA} expression was incomplete, demonstrating that either LgCam is so effective at inhibiting the JAK-STAT pathway that its virulence mechanism can even perturb heightened pathway activity or that hemocyte-specific inhibition of JAK-STAT activity is not the sole mechanism of LgCam virulence. Instead, the inhibition of JAK-STAT signaling in the body wall muscle or the manipulation of distinct signaling pathways may also play important roles.

Our findings suggest that successful wasp parasites may be able to suppress host JAK-STAT signaling as a virulence strategy, either via preventing pathway activation by blocking upstream signaling mechanisms, or by directly inhibiting the core components of the JAK-STAT signaling pathway (Fig 6). To distinguish between these possibilities, we tested the ability of the parasitoid strains to inhibit the melanotic tumor phenotype resulting from the *hop*^{Tum} mutation. *hop*^{Tum} is a gain of function mutation in the

D. melanogaster JAK that renders its activation independent of upstream signaling [60,61]. We predicted that parasitoid strains that block the upstream activation of the JAK-STAT pathway would have no effect on the *hop*^{Tum} mutant phenotype, whereas strains that directly inhibit core JAK-STAT signaling components would suppress melanotic tumor formation. We found that strains of two species of virulent wasps, *L. guineaensis* and *G. xanthopoda*, not only limited JAK-STAT activity in hemocytes and body wall muscle, but also decreased the penetrance of the tumor phenotype in *hop*^{Tum} mutants. This suggests that *L. guineaensis* and *G. xanthopoda* virulence strategies likely target core components of the JAK-STAT pathway (Fig 6). This idea is supported by the finding that purified LgCam venom can inhibit *hop*^{Tum} activity in primary hemocyte cultures, in the absence of immune induction or extrinsic pathway activation (Fig 4C). Strains of the additional virulent parasitoid species *L. heterotoma, L. boulardi,* and *L. victoriae* limited JAK-STAT pathway activity in host immune tissues but had no effect on the penetrance of the *hop*^{Tum} phenotype. This suggests that these parasitoid strains may inhibit the upstream mechanisms leading to JAK-STAT activation (Fig 6).

In *D. melanogaster,* the JAK-STAT pathway is activated when the *dome* receptor binds to ligands from the *upd* cytokine family [52–56]. The virulence strategies of *L. heterotoma, L. boulardi,* and *L. victoriae* may therefore block pathway activation by impairing the expression or function of the *upd* proteins or by interfering with the ability of *dome* to bind its ligands or transduce the cytokine signal by activating *hop*. Previous studies of host gene expression found that there was no induction of expression of the *upd* genes following infection with either *L. heterotoma* strain Lh14 and *L. boulardi* strain Lb17 [64]. These cytokines are required for JAK-STAT pathway activation and the encapsulation of parasitoid eggs following infection [50], so the lack of *upd* induction

suggests that this is a possible mechanism for the JAK-STAT inhibition seen in *L. heterotoma* and *L. boulardi*.

It has been demonstrated that individual wasp strains employ very specific virulence strategies against *D. melanogaster* [31,34,92], and our findings suggest that this extends to their anti-JAK-STAT strategies as well. These mechanisms of interference should be investigated further to better understand the ways that natural parasites may manipulate conserved signaling pathways involved in host immune responses. *D. melanogaster* is a widely used system for understanding JAK-STAT pathway functions. While there are four JAKs and seven STATs in the human system, *D. melanogaster* has only one JAK (*hop*) and one STAT (*Stat92E*), providing a much simpler system, but one with similar functionality and sequence conservation to the human JAK-STAT pathway [8,97]. Since its discovery more than twenty years ago, the JAK-STAT pathway has been shown to play an essential role in mammalian hematopoiesis similar to the mechanisms by which JAK-STAT signaling regulates cellular differentiation in *D. melanogaster*. *D. melanogaster* and the *Drosophila*-infecting parasitoid wasps thus provide an excellent model system to study the highly conserved JAK-STAT signaling pathway *in vivo*.

MATERIALS AND METHODS

Insects

Flies were maintained on standard Drosophila medium of cornmeal, yeast, and molasses. The *He-Gal4* (BDSC_8699), *C833-Gal4* (BDSC_6988), *Dot-Gal4* (BDSC_6903), *unc-5*^{GMR93E08} (*MZ-Gal4;* BDSC_48001), *w*^{1118} (BDSC_5905) and *hop*^{Tum}

(BDSC_8492) strains were obtained from the Bloomington Drosophila Stock Center (Bloomington, IN) (RRID:SCR_006457). *Mef2-Gal4* (BDSC_27390) was provided by Dr. A. Vrailas-Mortimer [98]. The constitutively active *Stat92E* transgene w^{1118};*UAS-Stat92E*$^{\Delta N \Delta C}$ (referred to as *UAS-Stat92E*^{CA}) [63] and the JAK-STAT reporter strain *10xSTAT92E-GFP* (BDSC_26197) [76] were provided by Dr. E. Bach. Wasp strains (Fig S2) were obtained and maintained as described in [78]. Briefly, all wasps were maintained on the *D. melanogaster* strain Canton S, with the exception of avirulent strains LcNet and LmAtl, which were maintained on *D. virilis*. Strain LbG486 was provided by Dr. D. Hultmark, LcNet was provided by Dr J. van Alphen, GxUg, LgCam and LgSA were provided by Dr. J. Pool. All other wasp strains were collected by the Schlenke lab.

Hemocyte counts

All crosses and experiments were carried out at 25ºC with the exception of experiments carried out with *hop*^{Tum} temperature sensitive mutants, which were incubated at 28ºC for up to 72 hours after a 24-hour wasp infection at 25ºC. For *Stat92E*^{CA} expression hemocyte counts, crosses between *Gal4* virgin females and *UAS-Stat92E*^{CA} or w^{1118} (wild type control) males were done at 25ºC, in three replicates per treatment. Wandering third instar larvae were selected for hemocyte counts. For *hop*^{Tum} hemocyte counts, flies were allowed to lay eggs for 24 hours at 25ºC. Egg lay plates were then placed at 28ºC and incubated for 48 hours. Thirty early third instar larvae were picked from egg lay plates and transferred to 35mm diameter Petri dishes, in three replicates per treatment. For infection treatments, three female wasps were allowed to oviposit for 24 hours at 25ºC. Following wasp infection, wasps were removed and the infected and control naïve larvae were shifted to 28ºC. Hemocytes were counted at 24

and 48 hours after being moved to 28ºC. From each cross, three sets of 5 larvae were bled into 20 µL of 1X Phosphate Buffered Saline (PBS), pH 7.4 with 0.01% PTU (to prevent blood cell lysis and melanization). The hemolymph dilution was transferred to a disposable hemocytometer (Incyto C-Chip DHC-N01). Hemocytes from sixteen 0.25 x 0.25 x 0.1 mm squares were counted for each replicate.

Imaging

Wasp infections of *10xSTAT92E-GFP* reporter flies were carried out as described above at 25ºC, and imaging took place 24 and 48 hours after wasp infection. Five larvae were dissected under immersion oil from each of three replicate plates. For quantification of *10xSTAT92E-GFP* corrected total cell fluorescence, 20 blood cells from each of the 5 larvae were analyzed for fluorescence in comparison to background using ImageJ software [12]. hop^{Tum} flies were imaged as pupae after 72 hours of incubation at 28ºC following wasp infection to allow adequate time for development of the tumor phenotype. Penetrance was determined by phenotyping larvae for presence or absence of melanotic tumors.

Wasp encapsulation

To measure wasp egg encapsulation ability, 30 late second instar larvae were placed on 35mm Petri dishes filled with standard Drosophila medium together with 3 female wasps at 25°C. Larvae were dissected 72hpi and the number of encapsulated eggs and hatched wasp larvae were counted. Experiments were performed in triplicate.

Venom purification

To separate the effects of venom activity from the infection and immune response process, venom was purified from dissected venom apparatuses as described in [99]. Briefly, dissected venom apparatuses were homogenized on ice in non-lysing conditions in 1X PBS, pH 7.4, supplemented with 0.5 mM EDTA and 1X Halt protease inhibitor cocktail (Thermo Scientific). Venom apparatus cells were pelleted by centrifugation at 12000 *g* at 4°C, and the supernatant containing venom was used to assess activity.

Ex vivo venom assays

To assess the ability of parasitoid venom to inhibit host JAK-STAT signaling, *hop*^{Tum}*;10xSTAT92E-GFP* larvae were raised at 28°C and dissected to establish primary hemocyte cultures. Third instar larvae were dissected into 1X PBS, pH7.4, with 0.01% PTU in multi well slides (Tekdon). Primary hemocyte cultures were mixed with 10 wasp equivalents of venom or PBS control and transferred into Tali Cellular Analysis slides (Invitrogen). After a 1-hour incubation period, GFP fluorescence intensity was determined using a Tali Image-Based Cytometer (Invitrogen) as described in [71].

Statistics

Welch two sample t-tests were used to compare immune cell count data between *UAS-Stat92E*^{CA} and *w*^{1118} crossed to each *Gal4* driver. To look for changes in the distribution of immune cell types, we used the χ^2 test. For each *Gal4* driver, the proportion of each hemocyte type in the control *w*^{1118} cross used as the probability estimate and p values were simulated using 2000 replicates [100]. χ^2 standardized

residuals were plotted for each cell type in each comparison to estimate the contribution of cell type to the overall χ^2 value. Residuals > |2| suggest a significant impact on the score [101].

Corrected total cell fluorescence values were analyzed by Analysis of Variance (ANOVA) followed by Dunnett's test for pairwise comparisons to the naïve control or LcNet infected larvae as indicated in the text. To analyze *hop*^{Tum} phenotypic penetrance data, we used generalized linear models with quasibinomial errors. Dunnett's test was used for pairwise comparisons to the control genotype. The proportion of encapsulated parasitoid eggs was compared between genotypes using the Analysis of Variance of Aligned Rank Transformed Data test. Correlation coefficients (ρ) between hemocyte concentrations and the penetrance of the *hop*^{Tum} melanotic tumor phenotype were calculated using Spearman's rank correlation. Mixed linear models, with replicate as a random effect, were used to test for differences in *10xSTAT92E-GFP* fluorescence intensity between venom and control treated primary hemocyte cultures.

All statistics were done in the R statistical computing environment [100] using the plyr [102], reshape2 [103], multcomp [104], ARTool [105], lme4 [106], lmerTest [107], and effects [108] packages. Graphs were produced using the ggplot2 and ggpubr packages [109,110].

Phylogenetics

Phylogenetic analyses were conducted in MEGA X [111,112] using COI DNA sequences for the parasitoid strains used in the study (Supplemental Table 1). Evolutionary history was inferred by using the Maximum Likelihood method and Kimura

2-parameter model with 1000 bootstrap replicates [113]. The initial tree for the heuristic search was obtained automatically by applying Neighbor-Join and BioNJ algorithms to a matrix of pairwise distances estimated using the Maximum Composite Likelihood (MCL) approach in MEGA X, and then selecting the topology with superior log likelihood value. Branches corresponding to partitions reproduced in less than 50% of the bootstrap replicates were collapsed. All positions containing gaps and missing data were eliminated. The resulting phylogenetic trees were visualized using FigTree (version 1.4.3, http://tree.bio.ed.ac.uk/).

Acknowledgments

We thank members of the Mortimer lab for comments on the manuscript, Drs. Alysia Vrailas-Mortimer and Erika Bach for *D. melanogaster* stocks, and Drs. Dan Hultmark, Jacques van Alphen and J. Pool for parasitoid strains. Research reported in this publication was supported by NIH Awards R35GM133760 to NTM and R01AI081879 to TAS. Stocks obtained from the Bloomington Drosophila Stock Center (NIH P40OD018537) were used in this study. The ISU Confocal Microscopy Facility was funded by NSF grant DBI-1828136.

Figure Legends

Fig 1. *Drosophila melanogaster* JAK-STAT signaling pathway activity is induced in immune tissues following wasp infection.

(A) A schematic to illustrate the *D. melanogaster* JAK-STAT pathway. The pathway can be activated by the interaction between *upd* and *dome* or by gain of function mutations in *hop* or *Stat92E*. The *10XStat92E-GFP* transgene expression serves as a readout of pathway activity. (B-I) GFP expression in *10XStat92E-GFP* larval hemocytes (B,F: brightfield, C,G: GFP), fat body (D,H) and body wall muscle (E,I) was imaged 48 hours following infection by the avirulent wasp *L. clavipes* (strain LcNet; F-I) and in age-matched naïve larvae (B-E). *10XStat92E-GFP* activity is induced in hemocytes (compare C vs G), fat body (D vs H) and body wall muscle (E vs I) following LcNet infection.

Fig 2. JAK-STAT activity in immune tissues is sufficient for lamellocyte production.

(A) The total number of circulating hemocytes from larvae expressing a constitutively active form of *Stat92E* (*Stat92E*^{CA}, black) compared to a *w*^{1118} control cross (cyan). Data are expressed as mean hemocyte number ± standard error of three replicates. Hemocyte numbers only changed significantly when *Stat92E*^{CA} was expressed body wall muscle (*Mef2-Gal4*). (B) Lamellocyte numbers from larvae expressing a constitutively active form of *Stat92E* (*Stat92E*^{CA}, black) compared to *w*^{1118} controls (cyan). Data are expressed as mean lamellocyte number ± standard error of three replicates. Lamellocyte numbers changed significantly when *Stat92E*^{CA} was expressed in hemocytes (*He-Gal4*), muscles (*Mef2-Gal4*) or fat body (*C833-Gal4*), but not when expressed in the posterior signaling center (*Dot-Gal4*) or medullary zone (*MZ-Gal4*) of the lymph gland. For A-B, * indicates $p < 0.05$ compared to the respective *w*^{1118} control cross by Welch two sample t-

test. (C) χ^2 standardized residuals plotted for plasmatocytes (cyan), prelamellocytes (magenta) and lamellocytes (black) following expression of *Stat92E*^{CA} in each tissue. Hemocyte concentrations were significantly altered by *Stat92E*^{CA} expression in hemocytes, fat body and body wall muscle. * indicates $p < 0.05$ compared to the respective *w*^{1118} control cross by χ^2 test.

Fig 3. GFP fluorescence is altered in *10XStat92E-GFP* hemocytes following wasp infection by multiple wasp strains.

GFP intensity measured as corrected total cell fluorescence in *10XStat92E-GFP* hemocytes at (A) 24 and (B) 48 hours post infection. Avirulent wasps LcNet and LmAtl induce the highest GFP fluorescence in comparison to multiple virulent wasp strains. Each data point represents the average corrected total cell fluorescence ± standard error for three replicates of 180 blood cells. * $p < 0.05$ compared to naïve control by Dunnett's test.

Fig 4. Wasp virulence strategies target host encapsulation ability downstream of JAK.

(A) The *hop*^{Tum} melanotic tumor phenotype observed in a mutant pupa. (B) Penetrance of *hop*^{Tum} phenotype 72 hours after wasp infection and in age-matched naïve control. Each data point represents the average penetrance ± standard error of three replicates of thirty observed pupae. * $p < 0.05$ compared to naïve control by Dunnett's test. (C) Calculated relative fluorescence intensity of GFP in primary hemocytes isolated from *hop*^{Tum}; *10XStat92E-GFP* larvae and incubated with LgCam venom or PBS control. Data are displayed as the mean fit (point) of the effect of incubation on fluorescence intensity ± standard error. * $p < 0.05$ compared to PBS control treated hemocytes by Analysis of Variance. (D) Encapsulation of LgCam eggs in larvae expressing *Stat92E*^{CA} in

hemocytes compared to w^{1118} control cross. Data are expressed as mean proportion encapsulated ± standard error of three replicates. * $p < 0.05$ compared to w^{1118} control cross by Analysis of Variance of Aligned Rank Transformed Data test. (E-F) Total count of circulating hemocytes (E) and lamellocyte number (F) in hop^{Tum} naïve larvae (cyan) or hop^{Tum} larvae infected by the indicated parasitoid (black). Data are expressed as mean (E) hemocyte or (F) lamellocyte number ± standard error of three replicates. * indicates $p < 0.05$ compared to naïve larvae by Welch two sample t-test.

Fig 5. Correlations between relative hemocyte counts and tumor penetrance in wasp-infected flies.

Scatterplots of relative counts of (A) plasmatocytes, (B) prelamellocytes, and (C) lamellocytes quantified 48hpi plotted against the penetrance of the hop^{Tum} melanotic tumor phenotype following infection or in age-matched naïve larvae. Data are shown for hop^{Tum} mutants infected by each wasp strain and naïve controls. The linear regression line for each correlation was calculated and plotted. 95% confidence intervals are shaded in gray. Plasmatocyte and prelamellocyte proportions do not correlate with percent tumor penetrance. In contrast, relative lamellocyte numbers are positively correlated with percent tumor penetrance.

Fig 6. *Drosophila*-infecting parasitoids inhibit the host JAK-STAT pathway.

Schematic illustrating the phases of JAK-STAT signal transduction: upstream activation, core signaling components, and signaling outputs including *10XStat92E-GFP* expression, and the phase of pathway activity inhibited by each parasitoid species we screened. For each species, the different strains appear to act at the same phase, so only species names are given for simplicity.

References

1. Kimbrell DA, Beutler B. The evolution and genetics of innate immunity. Nat Rev Genet. 2001;2: 256–267. doi:10.1038/35066006

2. Hoffmann JA, Kafatos FC, Janeway CA, Ezekowitz RA. Phylogenetic perspectives in innate immunity. Science. 1999;284: 1313–1318. doi:10.1126/science.284.5418.1313

3. Silverman N, Maniatis T. NF-κB signaling pathways in mammalian and insect innate immunity. Genes Dev. 2001;15: 2321–2342. doi:10.1101/gad.909001

4. Medzhitov R. Toll-like receptors and innate immunity. Nat Rev Immunol. 2001;1: 135–145. doi:10.1038/35100529

5. Imler JL, Hoffmann JA. Toll receptors in innate immunity. Trends Cell Biol. 2001;11: 304–311.

6. Lemaitre B, Nicolas E, Michaut L, Reichhart J-M, Hoffmann JA. The dorsoventral regulatory gene cassette spätzle/Toll/cactus controls the potent antifungal response in *Drosophila* adults. Cell. 1996;86: 973–983. doi:10.1016/S0092-8674(00)80172-5

7. Valanne S, Wang J-H, Rämet M. The *Drosophila* Toll signaling pathway. J Immunol Baltim Md 1950. 2011;186: 649–656. doi:10.4049/jimmunol.1002302

8. Agaisse H, Perrimon N. The roles of JAK/STAT signaling in *Drosophila* immune responses. Immunol Rev. 2004;198: 72–82.

9. Villarino AV, Kanno Y, Ferdinand JR, O'Shea JJ. Mechanisms of Jak/STAT signaling in immunity and disease. J Immunol. 2015;194: 21–27. doi:10.4049/jimmunol.1401867

10. Delaney JR, Stöven S, Uvell H, Anderson KV, Engström Y, Mlodzik M. Cooperative control of *Drosophila* immune responses by the JNK and NF-κB signaling pathways. EMBO J. 2006;25: 3068–3077. doi:10.1038/sj.emboj.7601182

11. Arthur JSC, Ley SC. Mitogen-activated protein kinases in innate immunity. Nat Rev Immunol. 2013;13: 679–692. doi:10.1038/nri3495

12. Mortimer NT, Goecks J, Kacsoh BZ, Mobley JA, Bowersock GJ, Taylor J, et al. Parasitoid wasp venom SERCA regulates *Drosophila* calcium levels and inhibits cellular immunity. Proc Natl Acad Sci. 2013;110: 9427–9432. doi:10.1073/pnas.1222351110

13. Vig M, Kinet J-P. Calcium signaling in immune cells. Nat Immunol. 2009;10: 21–27. doi:10.1038/ni.f.220

14. Boutros M, Agaisse H, Perrimon N. Sequential activation of signaling pathways during innate immune responses in *Drosophila*. Dev Cell. 2002;3: 711–722. doi:10.1016/S1534-5807(02)00325-8

15. Thaiss CA, Levy M, Itav S, Elinav E. Integration of innate immune signaling. Trends Immunol. 2016;37: 84–101. doi:10.1016/j.it.2015.12.003

16. Leiding JW, Ballow M. Precision medicine in the treatment of primary immunodeficiency diseases. Curr Opin Allergy Clin Immunol. 2018;18: 159–166. doi:10.1097/ACI.0000000000000431

17. Yazdani R, Abolhassani H, Rezaei N, Azizi G, Hammarström L, Aghamohammadi A. Evaluation of known defective signaling-associated molecules in patients who primarily diagnosed as Common Variable Immunodeficiency. Int Rev Immunol. 2016;35: 7–24. doi:10.3109/08830185.2015.1136306

18. Arjunaraja S, Snow AL. Gain-of-function mutations and immunodeficiency: at a loss for proper tuning of lymphocyte signaling. Curr Opin Allergy Clin Immunol. 2015;15: 533–538. doi:10.1097/ACI.0000000000000217

19. McGuire VA, Arthur JSC. Subverting Toll-Like Receptor signaling by bacterial pathogens. Front Immunol. 2015;6. doi:10.3389/fimmu.2015.00607

20. Schmid-Hempel P. Immune defence, parasite evasion strategies and their relevance for 'macroscopic phenomena' such as virulence. Philos Trans R Soc B Biol Sci. 2009;364: 85–98. doi:10.1098/rstb.2008.0157

21. Mitchell TJ. Molecular basis of virulence. Arch Dis Child. 1998;78: 197–200. doi:10.1136/adc.78.3.197

22. Jones RM, Wu H, Wentworth C, Luo L, Collier-Hyams L, Neish AS. *Salmonella* AvrA coordinates suppression of host immune and apoptotic defenses via JNK pathway blockade. Cell Host Microbe. 2008;3: 233–244. doi:10.1016/j.chom.2008.02.016

23. Royan SV, Jones RM, Koutsouris A, Roxas JL, Falzari K, Weflen AW, et al. Enteropathogenic *E. coli* non-LEE encoded effectors NleH1 and NleH2 attenuate NF-κB activation. Mol Microbiol. 2010;78: 1232–1245. doi:10.1111/j.1365-2958.2010.07400.x

24. West C, Rus F, Chen Y, Kleino A, Gangloff M, Gammon DB, et al. IIV-6 inhibits NF-κB responses in *Drosophila*. Viruses. 2019;11. doi:10.3390/v11050409

25. Thoetkiattikul H, Beck MH, Strand MR. Inhibitor κB-like proteins from a polydnavirus inhibit NF-κB activation and suppress the insect immune response. Proc Natl Acad Sci U S A. 2005;102: 11426–11431. doi:10.1073/pnas.0505240102

26. Colinet D, Schmitz A, Depoix D, Crochard D, Poirié M. Convergent use of RhoGAP toxins by eukaryotic parasites and bacterial pathogens. PLOS Pathog. 2007;3: e203. doi:10.1371/journal.ppat.0030203

27. Lemaitre B, Hoffmann J. The host defense of *Drosophila melanogaster*. Annu Rev Immunol. 2007;25: 697–743. doi:10.1146/annurev.immunol.25.022106.141615

28. Williams MJ. *Drosophila* hemopoiesis and cellular immunity. J Immunol Baltim Md 1950. 2007;178: 4711–4716.

29. Parsons B, Foley E. Cellular immune defenses of *Drosophila melanogaster*. Dev Comp Immunol. 2016;58: 95–101. doi:10.1016/j.dci.2015.12.019

30. Brennan CA, Anderson KV. *Drosophila*: The genetics of innate immune recognition and response. Annu Rev Immunol. 2004;22: 457–483. doi:10.1146/annurev.immunol.22.012703.104626

31. Dubuffet A, Colinet D, Anselme C, Dupas S, Carton Y, Poirié M. Variation of *Leptopilina boulardi* success in *Drosophila* hosts: What is inside the black box? In: Parasitology B-A in, editor. Academic Press; 2009. pp. 147–188.

32. Kim-Jo C, Gatti J-L, Poirié M. *Drosophila* cellular immunity against parasitoid wasps: A complex and time-dependent process. Front Physiol. 2019;10: 603. doi:10.3389/fphys.2019.00603

33. Carton Y, Bouletreau M, Van Alphen JJM, Van Lenteren JC. The *Drosophila* parasitic wasps. 3rd ed. The Genetics and Biology of *Drosophila*. 3rd ed. London: Academic Press; 1986.

34. Mathé-Hubert H, Kremmer L, Colinet D, Gatti J-L, Van Baaren J, Delava É, et al. Variation in the venom of parasitic wasps, drift, or selection? Insights From a multivariate QST analysis. Front Ecol Evol. 2019;7. doi:10.3389/fevo.2019.00156

35. Mortimer NT. Parasitoid wasp virulence: A window into fly immunity. Fly (Austin). 2013;7: 242–248. doi:10.4161/fly.26484

36. Carton Y, Nappi AJ. *Drosophila* cellular immunity against parasitoids. Parasitol Today. 1997;13: 218–227.

37. Russo J, Dupas S, Frey F, Carton Y, Brehelin M. Insect immunity: early events in the encapsulation process of parasitoid (*Leptopilina boulardi*) eggs in resistant and susceptible strains of *Drosophila*. Parasitology. 1996;112 (Pt 1): 135–142. doi:10.1017/s0031182000065173

38. Rizki TM, Rizki RM. Lamellocyte differentiation in *Drosophila* larvae parasitized by *Leptopilina*. Dev Comp Immunol. 1992;16: 103–110. doi:10.1016/0145-305x(92)90011-z

39. Anderl I, Vesala L, Ihalainen TO, Vanha-aho L-M, Andó I, Rämet M, et al. Transdifferentiation and proliferation in two distinct hemocyte lineages in *Drosophila melanogaster* larvae after wasp infection. PLOS Pathog. 2016;12: e1005746. doi:10.1371/journal.ppat.1005746

40. Honti V, Csordás G, Márkus R, Kurucz E, Jankovics F, Andó I. Cell lineage tracing reveals the plasticity of the hemocyte lineages and of the hematopoietic compartments in *Drosophila melanogaster*. Mol Immunol. 2010;47: 1997–2004. doi:10.1016/j.molimm.2010.04.017

41. Lanot R, Zachary D, Holder F, Meister M. Postembryonic hematopoiesis in *Drosophila*. Dev Biol. 2001;230: 243–257. doi:10.1006/dbio.2000.0123

42. Márkus R, Laurinyecz B, Kurucz E, Honti V, Bajusz I, Sipos B, et al. Sessile hemocytes as a hematopoietic compartment in *Drosophila melanogaster*. Proc Natl Acad Sci U S A. 2009;106: 4805–4809. doi:10.1073/pnas.0801766106

43. Rizki MTM. Alterations in the haemocyte population of *Drosophila melanogaster*. J Morphol. 1957;100: 437–458. doi:10.1002/jmor.1051000303

44. Tattikota SG, Cho B, Liu Y, Hu Y, Barrera V, Steinbaugh MJ, et al. A single-cell survey of *Drosophila* blood. Lemaître B, Akhmanova A, Lemaître B, editors. eLife. 2020;9: e54818. doi:10.7554/eLife.54818

45. Stofanko M, Kwon SY, Badenhorst P. Lineage tracing of lamellocytes demonstrates *Drosophila* macrophage plasticity. PloS One. 2010;5: e14051. doi:10.1371/journal.pone.0014051

46. Mortimer NT, Kacsoh BZ, Keebaugh ES, Schlenke TA. Mgat1-dependent N-glycosylation of membrane components primes *Drosophila melanogaster* blood cells for the cellular encapsulation response. PLoS Pathog. 2012;8: e1002819. doi:10.1371/journal.ppat.1002819

47. Carton Y, Poirié M, Nappi AJ. Insect immune resistance to parasitoids. Insect Sci. 2008;15: 67–87. doi:10.1111/j.1744-7917.2008.00188.x

48. Howell L, Sampson CJ, Xavier MJ, Bolukbasi E, Heck MMS, Williams MJ. A directed miniscreen for genes involved in the *Drosophila* anti-parasitoid immune response. Immunogenetics. 2012;64: 155–161. doi:10.1007/s00251-011-0571-3

49. Sorrentino RP, Melk JP, Govind S. Genetic analysis of contributions of Dorsal group and JAK-Stat92E pathway genes to larval hemocyte concentration and the egg encapsulation response in *Drosophila*. Genetics. 2004;166: 1343–1356. doi:10.1534/genetics.166.3.1343

50. Yang H, Kronhamn J, Ekström J-O, Korkut GG, Hultmark D. JAK/STAT signaling in *Drosophila* muscles controls the cellular immune response against parasitoid infection. EMBO Rep. 2015;16: 1664–1672. doi:10.15252/embr.201540277

51. Arbouzova NI, Zeidler MP. JAK/STAT signalling in *Drosophila*: Insights into conserved regulatory and cellular functions. Dev Camb Engl. 2006;133: 2605–2616. doi:10.1242/dev.02411

52. Harrison DA, McCoon PE, Binari R, Gilman M, Perrimon N. *Drosophila unpaired* encodes a secreted protein that activates the JAK signaling pathway. Genes Dev. 1998;12: 3252–3263. doi:10.1101/gad.12.20.3252

53. Chen H-W, Chen X, Oh S-W, Marinissen MJ, Gutkind JS, Hou SX. *mom* identifies a receptor for the *Drosophila* JAK/STAT signal transduction pathway and encodes a protein distantly related to the mammalian cytokine receptor family. Genes Dev. 2002;16: 388–398. doi:10.1101/gad.955202

54. Hombría JC-G, Brown S, Häder S, Zeidler MP. Characterisation of Upd2, a *Drosophila* JAK/STAT pathway ligand. Dev Biol. 2005;288: 420–433. doi:10.1016/j.ydbio.2005.09.040

55. Wright VM, Vogt KL, Smythe E, Zeidler MP. Differential activities of the *Drosophila* JAK/STAT pathway ligands Upd, Upd2 and Upd3. Cell Signal. 2011;23: 920–927. doi:10.1016/j.cellsig.2011.01.020

56. Brown S, Hu N, Hombría JC. Identification of the first invertebrate interleukin JAK/STAT receptor, the *Drosophila* gene *domeless*. Curr Biol CB. 2001;11: 1700–1705. doi:10.1016/s0960-9822(01)00524-3

57. Hou XS, Melnick MB, Perrimon N. *marelle* acts downstream of the *Drosophila* HOP/JAK kinase and encodes a protein similar to the mammalian STATs. Cell. 1996;84: 411–419. doi:10.1016/S0092-8674(00)81286-6

58. Yan R, Small S, Desplan C, Dearolf CR, Darnell JE. Identification of a STAT gene that functions in *Drosophila* development. Cell. 1996;84: 421–430. doi:10.1016/S0092-8674(00)81287-8

59. Kwon E-J, Park H-S, Kim Y-S, Oh E-J, Nishida Y, Matsukage A, et al. Transcriptional regulation of the *Drosophila raf* proto-oncogene by *Drosophila* STAT during development and in immune response. J Biol Chem. 2000;275: 19824–19830. doi:10.1074/jbc.M001114200

60. Luo H, Hanratty WP, Dearolf CR. An amino acid substitution in the *Drosophila hopTum-l* Jak kinase causes leukemia-like hematopoietic defects. EMBO J. 1995;14: 1412–1420.

61. Hanratty WP, Dearolf CR. The *Drosophila Tumorous-lethal* hematopoietic oncogene is a dominant mutation in the *hopscotch* locus. Mol Gen Genet MGG. 1993;238: 33–37.

62. Zettervall C-J, Anderl I, Williams MJ, Palmer R, Kurucz E, Ando I, et al. A directed screen for genes involved in *Drosophila* blood cell activation. Proc Natl Acad Sci U S A. 2004;101: 14192–14197. doi:10.1073/pnas.0403789101

63. Ekas LA, Cardozo TJ, Flaherty MS, McMillan EA, Gonsalves FC, Bach EA. Characterization of a dominant-active STAT that promotes tumorigenesis in *Drosophila*. Dev Biol. 2010;344: 621–636. doi:10.1016/j.ydbio.2010.05.497

64. Schlenke TA, Morales J, Govind S, Clark AG. Contrasting infection strategies in generalist and specialist wasp parasitoids of *Drosophila melanogaster*. PLOS Pathog. 2007;3: e158. doi:10.1371/journal.ppat.0030158

65. Furihata SX, Matsumoto H, Kimura MT, Hayakawa Y. Venom components of *Asobara japonica* impair cellular immune responses of host *Drosophila melanogaster*. Arch Insect Biochem Physiol. 2013;83: 86–100. doi:10.1002/arch.21093

66. Moreau SJM, Vinchon S, Cherqui A, Prévost G. Components of *Asobara* venoms and their effects on hosts. Adv Parasitol. 2009;70: 217–232. doi:10.1016/S0065-308X(09)70008-9

67. Colinet D, Dubuffet A, Cazes D, Moreau S, Drezen J-M, Poirié M. A serpin from the parasitoid wasp *Leptopilina boulardi* targets the *Drosophila* phenoloxidase cascade. Dev Comp Immunol. 2009;33: 681–689. doi:10.1016/j.dci.2008.11.013

68. Coulette Q, Lemauf S, Colinet D, Prévost G, Anselme C, Poirié M, et al. Biochemical characterization and comparison of aspartylglucosaminidases secreted in venom of the parasitoid wasps *Asobara tabida* and *Leptopilina heterotoma*. PLOS ONE. 2017;12: e0181940. doi:10.1371/journal.pone.0181940

69. Labrosse C, Stasiak K, Lesobre J, Grangeia A, Huguet E, Drezen JM, et al. A RhoGAP protein as a main immune suppressive factor in the *Leptopilina boulardi* (Hymenoptera, Figitidae)–*Drosophila melanogaster* interaction. Insect Biochem Mol Biol. 2005;35: 93–103. doi:10.1016/j.ibmb.2004.10.004

70. Moreau SJM, Eslin P, Giordanengo P, Doury G. Comparative study of the strategies evolved by two parasitoids of the genus *Asobara* to avoid the immune response of the host, *Drosophila melanogaster*. Dev Comp Immunol. 2003;27: 273–282. doi:10.1016/s0145-305x(02)00101-5

71. Trainor JE, Kr P, Mortimer NT. Immune cell production is targeted by parasitoid wasp virulence in a *Drosophila*–parasitoid wasp interaction. Pathogens. 2021;10: 49. doi:10.3390/pathogens10010049

72. Labrosse C, Eslin P, Doury G, Drezen JM, Poirié M. Haemocyte changes in *D. melanogaster* in response to long gland components of the parasitoid wasp *Leptopilina boulardi*: a Rho-GAP protein as an important factor. J Insect Physiol. 2005;51: 161–170. doi:10.1016/j.jinsphys.2004.10.004

73. Chiu H, Govind S. Natural infection of *D. melanogaster* by virulent parasitic wasps induces apoptotic depletion of hematopoietic precursors. Cell Death Differ. 2002;9: 1379–1381. doi:10.1038/sj.cdd.4401134

74. Rizki RM, Rizki TM. Parasitoid virus-like particles destroy *Drosophila* cellular immunity. Proc Natl Acad Sci U S A. 1990;87: 8388–8392. doi:10.1073/pnas.87.21.8388

75. Rizki TM, Rizki RM, Carton Y. *Leptopilina heterotoma* and *L. boulardi*: strategies to avoid cellular defense responses of *Drosophila melanogaster*. Exp Parasitol. 1990;70: 466–475. doi:10.1016/0014-4894(90)90131-u

76. Bach EA, Ekas LA, Ayala-Camargo A, Flaherty MS, Lee H, Perrimon N, et al. GFP reporters detect the activation of the *Drosophila* JAK/STAT pathway in vivo. Gene Expr Patterns GEP. 2007;7: 323–331. doi:10.1016/j.modgep.2006.08.003

77. Sorrentino RP, Carton Y, Govind S. Cellular immune response to parasite infection in the *Drosophila* lymph gland is developmentally regulated. Dev Biol. 2002;243: 65–80. doi:10.1006/dbio.2001.0542

78. Kacsoh BZ, Schlenke TA. High hemocyte load is associated with increased resistance against parasitoids in *Drosophila suzukii*, a relative of *D. melanogaster*. PloS One. 2012;7: e34721. doi:10.1371/journal.pone.0034721

79. Gerritsma S, Haan A de, Zande L van de, Wertheim B. Natural variation in differentiated hemocytes is related to parasitoid resistance in *Drosophila melanogaster*. J Insect Physiol. 2013;59: 148–158. doi:10.1016/j.jinsphys.2012.09.017

80. Prévost G, Eslin P. Hemocyte load and immune resistance to *Asobara tabida* are correlated in species of the *Drosophila melanogaster* subgroup. J Insect Physiol. 1998;44: 807–816. doi:10.1016/s0022-1910(98)00013-4

81. Brand AH, Perrimon N. Targeted gene expression as a means of altering cell fates and generating dominant phenotypes. Development. 1993;118: 401–415.

82. Hrdlicka L, Gibson M, Kiger A, Micchelli C, Schober M, Schöck F, et al. Analysis of twenty-four Gal4 lines in *Drosophila melanogaster*. genesis. 2002;34: 51–57. doi:10.1002/gene.10125

83. Haghighi AP, McCabe BD, Fetter RD, Palmer JE, Hom S, Goodman CS. Retrograde control of synaptic transmission by postsynaptic CaMKII at the *Drosophila* neuromuscular junction. Neuron. 2003;39: 255–267. doi:10.1016/S0896-6273(03)00427-6

84. Sinenko SA, Shim J, Banerjee U. Oxidative stress in the haematopoietic niche regulates the cellular immune response in *Drosophila*. EMBO Rep. 2012;13: 83–89. doi:10.1038/embor.2011.223

85. Tokusumi T, Tokusumi Y, Brahier M, Lam V, Stoller-Conrad J, Kroeger P, et al. Screening and analysis of Janelia FlyLight project enhancer-Gal4 strains identifies multiple gene enhancers active during hematopoiesis in normal and wasp-challenged *Drosophila* larvae. G3 Bethesda Md. 2017;7: 437–448. doi:10.1534/g3.116.034439

86. Makki R, Meister M, Pennetier D, Ubeda J-M, Braun A, Daburon V, et al. A short receptor downregulates JAK-STAT signalling to control the *Drosophila* cellular immune response. PLoS Biol. 2010;8. doi:10.1371/journal.pbio.1000441

87. Gao H, Wu X, Fossett N. Upregulation of the *Drosophila* Friend of GATA Gene *u-shaped* by JAK/STAT Signaling Maintains Lymph Gland Prohemocyte Potency. Mol Cell Biol. 2009;29: 6086–6096. doi:10.1128/MCB.00244-09

88. Rodrigues D, Renaud Y, VijayRaghavan K, Waltzer L, Inamdar MS. Differential activation of JAK-STAT signaling reveals functional compartmentalization in *Drosophila* blood progenitors. Shim J, editor. eLife. 2021;10: e61409. doi:10.7554/eLife.61409

89. Lue C-H, Driskell AC, Leips J, Buffington ML. Review of the genus *Leptopilina* (Hymenoptera, Cynipoidea, Figitidae, Eucoilinae) from the Eastern United States,

including three newly described species. J Hymenopt Res. 2016;53: 35–76. doi:10.3897/jhr.53.10369

90. Kacsoh BZ, Bozler J, Schlenke TA. A role for nematocytes in the cellular immune response of the drosophilid *Zaprionus indianus*. Parasitology. 2014;141: 697–715. doi:10.1017/s0031182013001431

91. Chui H, Sorrentino RP, Govind S. Suppression of the *Drosophila* cellular immune response by *Ganaspis xanthopoda*. In: Beck G, Sugumaran M, Cooper EL, editors. Phylogenetic Perspectives on the Vertebrate Immune System. Springer US; 2001. pp. 161–167. doi:10.1007/978-1-4615-1291-2_14

92. Cavigliasso F, Mathé-Hubert H, Kremmer L, Rebuf C, Gatti J-L, Malausa T, et al. Rapid and differential evolution of the venom composition of a parasitoid wasp depending on the host strain. Toxins. 2019;11. doi:10.3390/toxins11110629

93. Harrison DA, Binari R, Nahreini TS, Gilman M, Perrimon N. Activation of a *Drosophila* Janus kinase (JAK) causes hematopoietic neoplasia and developmental defects. EMBO J. 1995;14: 2857–2865.

94. Evans CJ, Hartenstein V, Banerjee U. Thicker than blood. Dev Cell. 2003;5: 673–690. doi:10.1016/S1534-5807(03)00335-6

95. Williams MJ, Wiklund M-L, Wikman S, Hultmark D. Rac1 signalling in the *Drosophila* larval cellular immune response. J Cell Sci. 2006;119: 2015–2024. doi:10.1242/jcs.02920

96. Ratheesh A, Belyaeva V, Siekhaus DE. *Drosophila* immune cell migration and adhesion during embryonic development and larval immune responses. Curr Opin Cell Biol. 2015;36: 71–79. doi:10.1016/j.ceb.2015.07.003

97. Zeidler MP, Bausek N. The *Drosophila* JAK-STAT pathway. JAK-STAT. 2013;2. doi:10.4161/jkst.25353

98. Vrailas-Mortimer A, del Rivero T, Mukherjee S, Nag S, Gaitanidis A, Kadas D, et al. A muscle-specific p38 MAPK/Mef2/MnSOD pathway regulates stress, motor function, and life span in *Drosophila*. Dev Cell. 2011;21: 783–795. doi:10.1016/j.devcel.2011.09.002

99. Goecks J, Mortimer NT, Mobley JA, Bowersock GJ, Taylor J, Schlenke TA. Integrative approach reveals composition of endoparasitoid wasp venoms. PLOS One. 2013;8: e64125. doi:10.1371/journal.pone.0064125

100. R Core Team. R: A language and environment for statistical computing. R Foundation for Statistical Computing, Vienna, Austria; 2021. Available: https://www.R-project.org

101. Sharpe D. Chi-square test is statistically significant: Now what? Pract Assess Res Eval. 2019;20. doi:https://doi.org/10.7275/tbfa-x148

102. Wickham H. The split-apply-combine strategy for data analysis. J Stat Softw. 2011;40: 1–29. doi:10.18637/jss.v040.i01

103. Wickham H. Reshaping data with the reshape package. J Stat Softw. 2007;21: 1–20. doi:10.18637/jss.v021.i12

104. Hothorn T, Bretz F, Westfall P. Simultaneous inference in general parametric models. Biom J Biom Z. 2008;50: 346–363. doi:10.1002/bimj.200810425

105. Wobbrock JO, Findlater L, Gergle D, Higgins JJ. The aligned rank transform for nonparametric factorial analyses using only anova procedures. Proceedings of the SIGCHI Conference on Human Factors in Computing Systems. Vancouver, BC, Canada: Association for Computing Machinery; 2011. pp. 143–146. doi:10.1145/1978942.1978963

106. Bates D, Mächler M, Bolker B, Walker S. Fitting linear mixed-effects models using lme4. J Stat Softw. 2015;67: 1–48. doi:10.18637/jss.v067.i01

107. Kuznetsova A, Brockhoff PB, Christensen RHB. lmerTest package: Tests in linear mixed effects models. J Stat Softw. 2017;82: 1–26. doi:10.18637/jss.v082.i13

108. Fox J, Weisberg S. Visualizing fit and lack of fit in complex regression models with predictor effect plots and partial residuals. J Stat Softw. 2018;87: 1–27. doi:10.18637/jss.v087.i09

109. Wickham H. ggplot2: Elegant graphics for data analysis. New York: Springer-Verlag; 2009. doi:10.1007/978-0-387-98141-3

110. Kassambara A. ggpubr: “ggplot2” based publication ready plots. 2020. Available: https://CRAN.R-project.org/package=ggpubr

111. Kumar S, Stecher G, Li M, Knyaz C, Tamura K. MEGA X: Molecular evolutionary genetics analysis across computing platforms. Mol Biol Evol. 2018;35: 1547–1549. doi:10.1093/molbev/msy096

112. Stecher G, Tamura K, Kumar S. Molecular Evolutionary Genetics Analysis (MEGA) for macOS. Mol Biol Evol. 2020 [cited 20 Feb 2020]. doi:10.1093/molbev/msz312

113. Kimura M. A simple method for estimating evolutionary rates of base substitutions through comparative studies of nucleotide sequences. J Mol Evol. 1980;16: 111–120. doi:10.1007/bf01731581

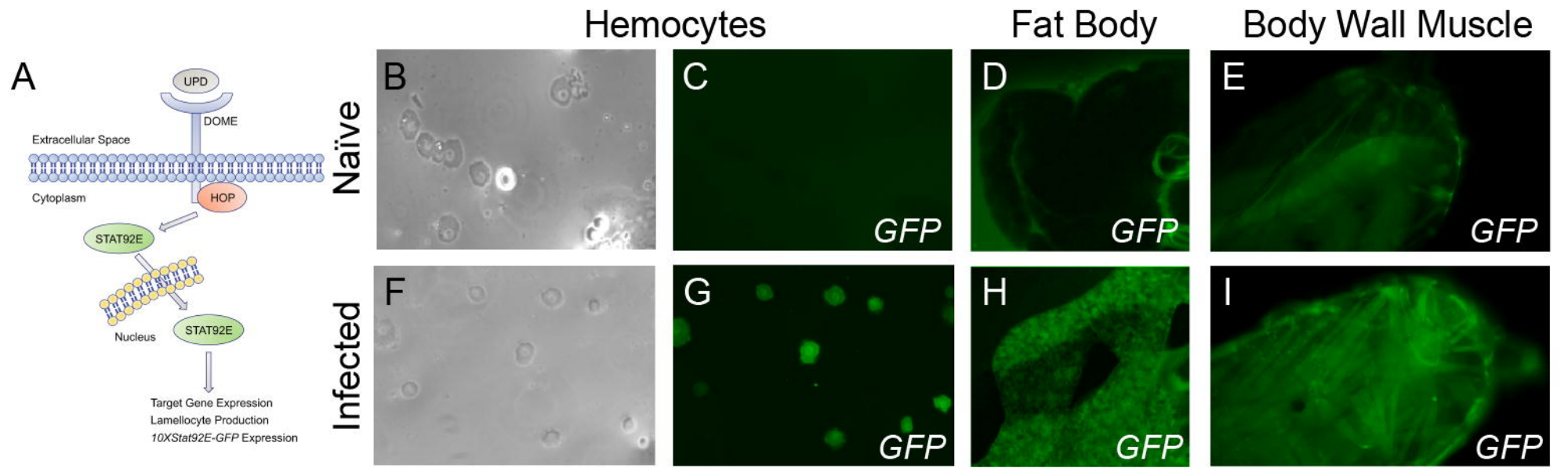
Hemocytes
Fat Body
Body Wall Muscle
A
UPD
DOME
Extracellular Space
Cytoplasm
HOP
STAT92E
Nucleus
STAT92E
Target Gene Expression
Lamellocyte Production
10XStat92E-GFP Expression
Naïve
Infected
B
C
D
E
F
G
H
I
GFP
GFP
GFP
GFP
GFP
GFP

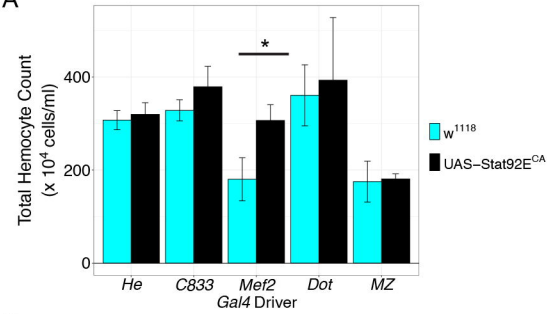
A
Total Hemocyte Count
(x 10^4 cells/ml)
400
200
0
*
He
C833
Mef2
Dot
MZ
Gal4 Driver
w1118
UAS−Stat92E^CA

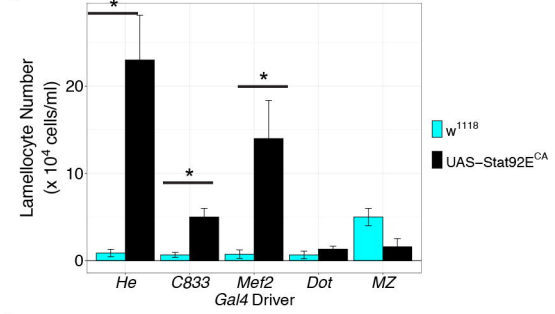
B
Lamellocyte Number
(x 10^4 cells/ml)
20
10
0
*
*
*
He
C833
Mef2
Dot
MZ
Gal4 Driver
w1118
UAS−Stat92E^CA

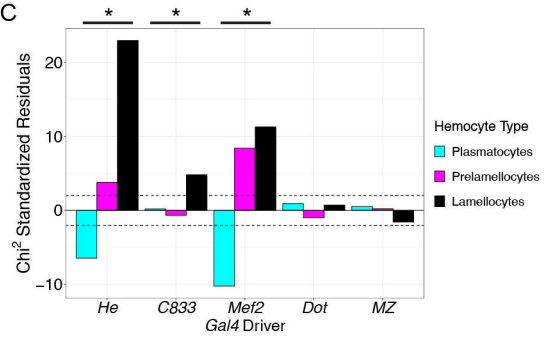
C
Chi2 Standardized Residuals
20
10
0
−10
*
*
*
He
C833
Mef2
Dot
MZ
Gal4 Driver
Hemocyte Type
Plasmatocytes
Prelamellocytes
Lamellocytes

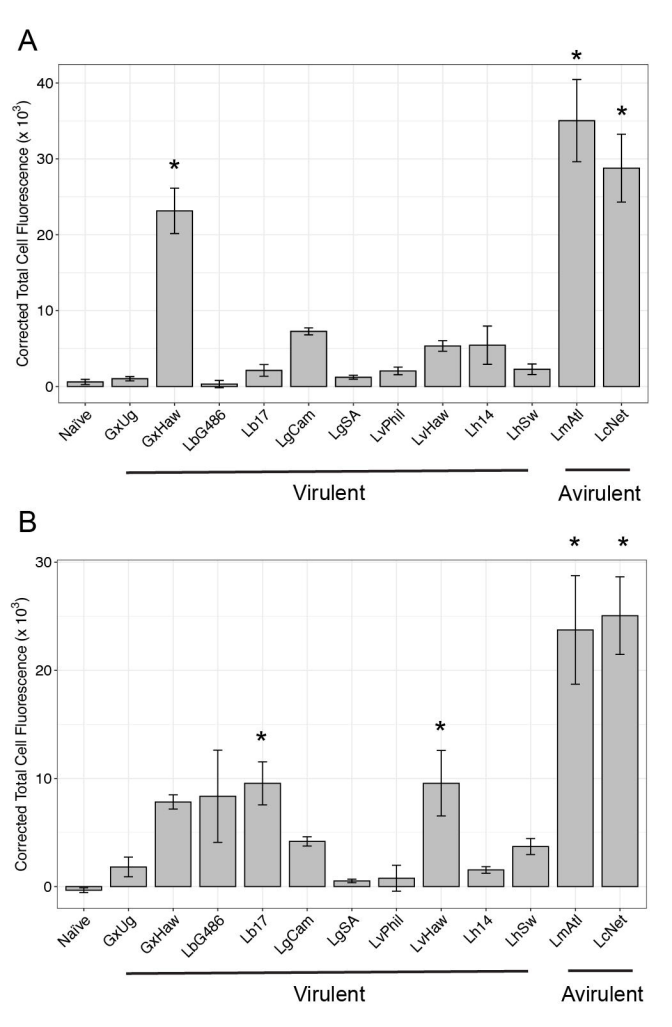
A
Corrected Total Cell Fluorescence (x 10^3)
40
30
20
10
0
*
*
*
Naïve
GxUg
GxHaw
LbG486
Lb17
LgCam
LgSA
LvPhil
LvHaw
Lh14
LhSw
LmAtl
LcNet
Virulent
Avirulent
B
Corrected Total Cell Fluorescence (x 10^3)
30
20
10
0
*
*
*
*
Naïve
GxUg
GxHaw
LbG486
Lb17
LgCam
LgSA
LvPhil
LvHaw
Lh14
LhSw
LmAtl
LcNet
Virulent
Avirulent

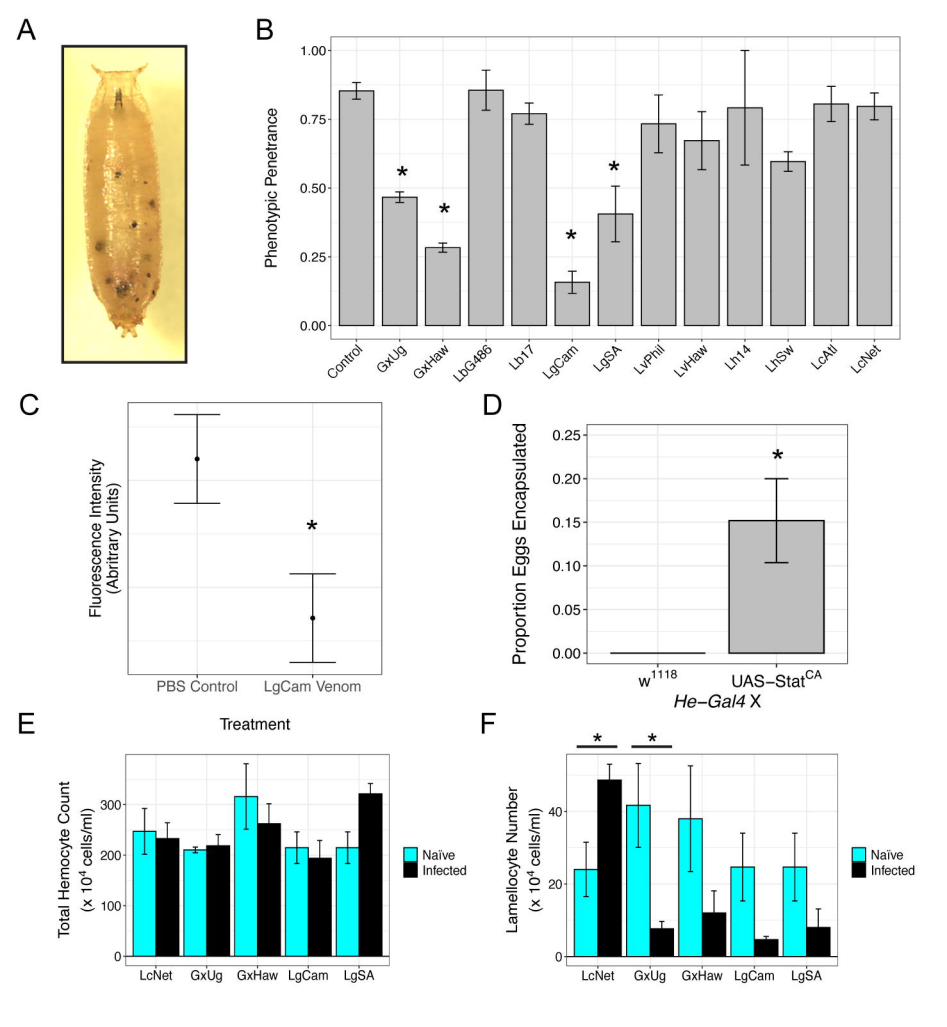
A
B
Phenotypic Penetrance
1.00
0.75
0.50
0.25
0.00
Control
GxUg
GxHaw
LbG486
Lb17
LgCam
LgSA
LvPhil
LvHaw
Lh14
LhSw
LcAtl
LcNet
C
Fluorescence Intensity
(Abritrary Units)
PBS Control
LgCam Venom
D
Proportion Eggs Encapsulated
0.25
0.20
0.15
0.10
0.05
0.00
w1118
UAS–StatCA
He–Gal4 X
E
Treatment
Total Hemocyte Count
(x 10^4 cells/ml)
300
200
100
0
LcNet
GxUg
GxHaw
LgCam
LgSA
Naïve
Infected
F
Lamellocyte Number
(x 10^4 cells/ml)
40
20
0
LcNet
GxUg
GxHaw
LgCam
LgSA
Naïve
Infected

A

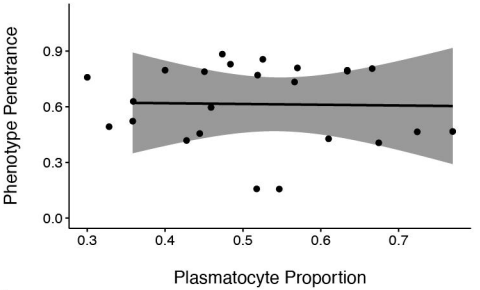
Phenotype Penetrance
0.0
0.3
0.6
0.9
0.3
0.4
0.5
0.6
0.7
Plasmatocyte Proportion

B

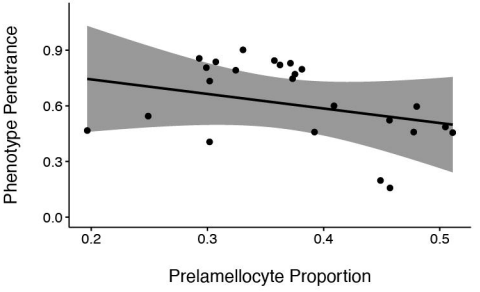
Phenotype Penetrance
0.0
0.3
0.6
0.9
0.2
0.3
0.4
0.5
Prelamellocyte Proportion

C

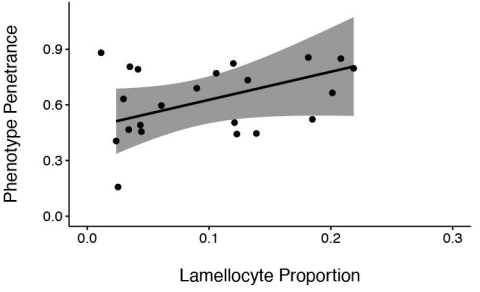
Phenotype Penetrance
0.0
0.3
0.6
0.9
0.0
0.1
0.2
0.3
Lamellocyte Proportion

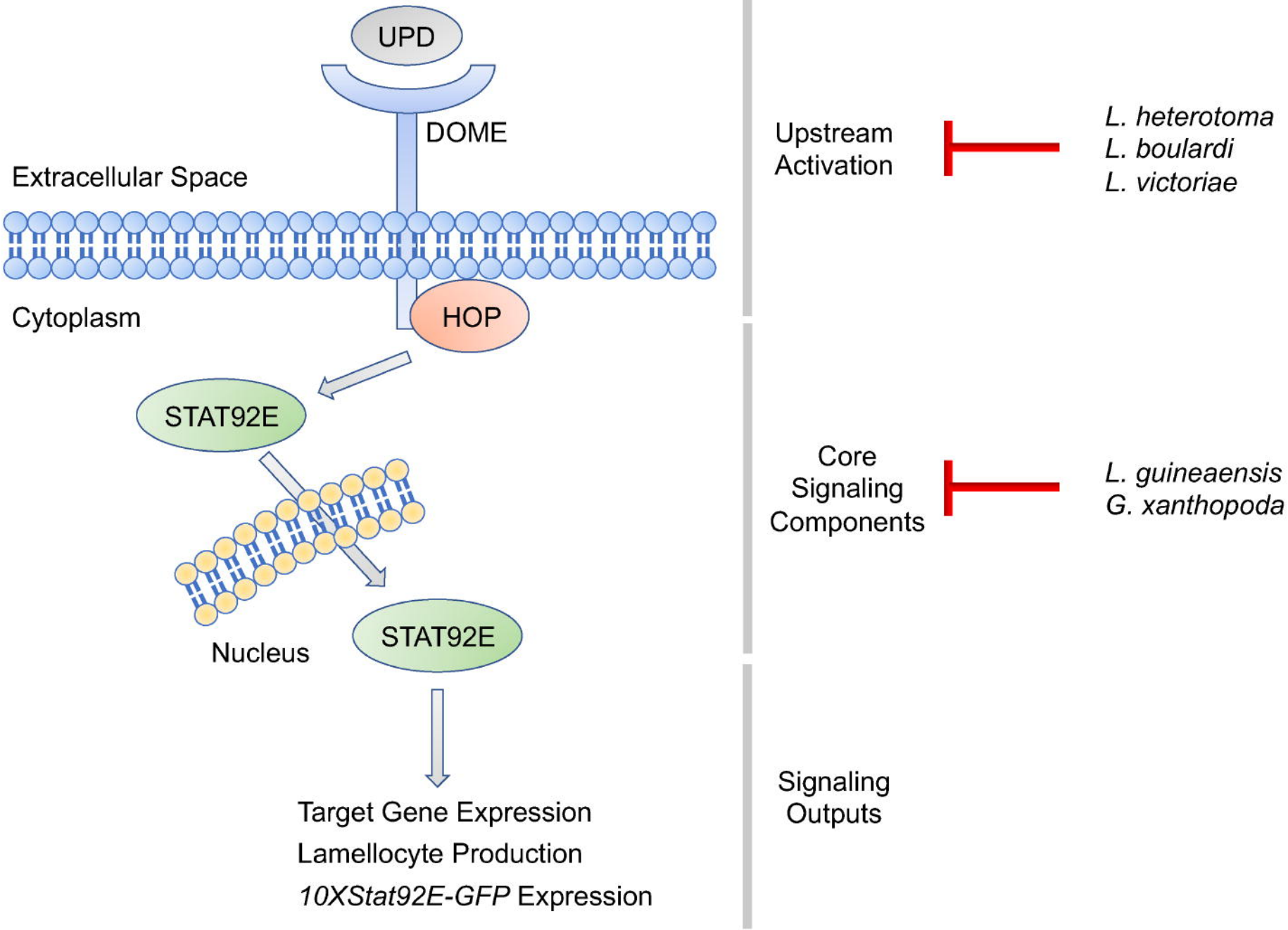
UPD
DOME
Extracellular Space
Cytoplasm
HOP
STAT92E
Nucleus
STAT92E
Target Gene Expression
Lamellocyte Production
10XStat92E-GFP Expression
Upstream Activation
L. heterotoma
L. boulardi
L. victoriae
Core Signaling Components
L. guineaensis
G. xanthopoda
Signaling Outputs